Abdom Imaging 23:431–436 (1998)

Abdominal Imaging

Enhancement patterns of renal masses during multiphase helical CT acquisitions

M. Garant,[1] **V. M. Bonaldi,**[1] **P. Taourel,**[1] **M. F. Pinsky,**[2] **P. M. Bret**[1]

[1]Department of Diagnostic Radiology, Montreal General Hospital, 1650 Cedar Avenue, Montreal, Quebec, H3G 1A4, Canada
[2]Department of Diagnostic Radiology, SMBD Jewish General Hospital, McGill University, 3755 Cote-Ste-Catherine Road, Montreal, Quebec H3T 1E2 Canada

Received: 6 December 1996/Accepted: 27 January 1997

Abstract

Background: To describe the appearance of renal masses during multiphase helical computed tomography (CT) acquisition and evaluate the impact of a cortical nephrographic phase on diagnosis.

Methods: The CT examinations of 33 patients with 37 lesions [18 renal cell carcinomas (RCC), nine solid tumors, 10 cystic lesions] were reviewed to characterize renal masses during four phases of CT scanning: plain, cortical nephrographic, tubular nephrographic, and pyelographic. Two reviewers analyzed all lesions on the complete data set, and a third reviewer analyzed three combinations of images separately: (1) plain and tubular nephrographic phases, (2) plain and cortical nephrographic phases, and (3) three phases combined. Receiver operating characteristics (ROC) curves were generated to determine the respective value of each combination in lesion characterization.

Results: During the cortical nephrographic phase, hyperdensity of solid renal masses was 100% specific and 22% sensitive for RCC, whereas combining hyperdense and isoattenuating heterogeneous masses was 91% specific and 56% sensitive. ROC curves demonstrated a sensitivity of 85%, 90%, 100% for the three combinations, respectively, with a constant specificity of 88% for diagnosing RCC.

Conclusion: The cortical nephrographic phase is useful to characterize renal masses and should be included in the routine helical CT protocol.

Key words: Kidney—mass—Computed tomography—Helical—Characterization.

Correspondence to: P. M. Bret

Computed tomography (CT) is considered to be the optimal imaging modality to detect and stage renal cell carcinoma (RCC) [1–7]. The diagnostic accuracy of CT is reported to be close to 95%. Characterization of a renal mass on CT relies on several factors, among which the definite demonstration of enhancement is the most significant [2–5, 8–14]. The standard accepted protocol for CT evaluation of renal masses consists of both plain and enhanced images, typically acquired during the tubular nephrographic phase of excretion of contrast material [2–4, 7, 10, 12, 14–18]. Before helical CT, characterization of a renal mass also often relied on a dynamic sequence performed at the level of the tumor, without incrementation [19]. However, with this technique, the information is limited to a single level, and there is a risk of misregistration artifact, especially for small tumors. Recently, investigators have evaluated the usefulness of helical CT in the detection of renal masses during the cortical nephrographic (corticomedullary), tubular nephrographic (nephrographic), and pyelographic phases of excretion of intravenous contrast [18, 20–23]. However, no study has specifically evaluated the value of an early cortical nephrographic phase acquisition in addition to the usual tubular nephrographic phase acquisition.

The purpose of this study was twofold. The first objective was to describe the appearance of renal masses during a multiphasic helical CT acquisition including plain, cortical nephrographic phase, tubular nephrographic phase, and pyelographic phase acquisitions. The second objective was to evaluate the value of an added cortical nephrographic phase acquisition to accurately diagnose RCC by using receiver operating characteristic (ROC) curves generated from data obtained after evaluation of three separate combinations of image sets: (1) plain and tu-

bular nephrographic phases combined, (2) plain and cortical nephrographic phases combined, and (3) all three phases combined.

Materials and methods

All CT examinations indicated to evaluate known renal masses and performed with helical multiphasic acquisition between May 1993 and July 1995 were reviewed to characterize the appearance of renal masses during four phases of CT acquisition: plain images, cortical nephrographic phase, tubular nephrographic phase, and pyelographic phase. From a total of 48 examinations, 15 were subsequently excluded: 12 patients were lost to follow-up, and three studies were technically suboptimal. The 33 remaining examinations were included in the study. The patient population included 18 women and 15 men, with a mean age of 60 years, and a range of 19–78 years. Twenty-nine patients had a single lesion, and four patients had bilateral lesions, for a total of 37 lesions.

The lesions were distributed as follows: 18 RCC, one urothelial transitional cell carcinoma, one metastasis from primary lung adenocarcinoma, one oncocytoma, four angiomyolipomas, two abscesses, three complicated renal cysts, and seven simple renal cysts. All diagnoses were confirmed by pathology (20 lesions), percutaneous biopsy (two lesions), history (one lesion), or a combination of imaging techniques with follow-up and correlative imaging studies (ultrasonography, magnetic resonance imaging: 14 lesions) [24–26]. The size of the lesions was distributed as follows: 16 lesions, including five RCC, measured less than 3 cm; 12 lesions, including six RCC, measured between 3 and 5 cm; and nine lesions, including seven RCC, were more than 5 cm.

The CT examinations were performed with a Toshiba TCT 900 SX (Toshiba Medical Systems, Tustin, CA). All patients were given intravenous contrast. Both ionic (n = 17) and nonionic (n = 16) contrast media were used according to our institutional guidelines on the use of nonionic contrast material. All injections were performed from an antecubital venous approach, with the use of a power injector (MCT 200, Medrad, Pittsburgh, PA). The volume of injected intravenous contrast was calculated according to the patient's weight, with a mean volume of 1.91 mL per kilogram (range = 1.2–2.25 mL/kg) and a mean total quantity of delivered iodine of 43.6 g per patient (average = 0.56 g/kg). The mean rate of injection was 5.8 mL per second (range = 3–6 mL/s). The delays between the initiation of the injection and the initiation of the cortical nephrographic and tubular nephrographic phase acquisitions were 20.5 s (range = 15–30 s) and 76.3 s (range = 54–109 s), respectively. The pyelographic phase acquisition was available for 27 renal lesions. Images of the lesions during all phases were photographed by using a window level and width of 30 HU and 400 HU, respectively, and printed on separate sheets (15 images/sheet) with a digital camera system. For all 37 lesions, several density measurements were made available to the reviewers on hard copies. Information regarding the patient's identity was removed.

Three reviewers, specializing in abdominal imaging and blinded to the clinical symptoms, to other imaging studies, and to the final outcome, contributed to the study. Two reviewers were provided with the complete sets of images and independently analyzed all lesions to collect detailed information relative to the appearance of each individual lesion at all phases of acquisition [4, 10, 11]. Lesions with cystic components were separated from the solid ones and described according to standard guidelines [11]. Data were recorded on a data sheet for each lesion. A third independent reviewer analyzed three combinations of images separately: (1) plain and tubular nephrographic phases combined, (2) plain and cortical nephrographic phases combined, and (3) all three phases combined. The sets of images were presented randomly, with each review session being scheduled with at least a 1-week time interval. The reviewer was asked to assign a score relating to the likelihood of RCC of each renal mass: 1 = definitely benign, 2 = probably benign, 3 = indeterminate, 4 = probably malignant, and 5 = definitely malignant. ROC curves were generated from this data to determine the respective value of each combination of phases in the characterization of RCC.

Results

Twenty-six of the 37 lesions appeared diffusely solid, including 17 RCC, one urothelial transitional cell carcinoma, one metastasis from primary lung adenocarcinoma, one oncocytoma, four angiomyolipomas, and two abscesses. The 11 remaining lesions either appeared to be cystic or had a cystic component and included one RCC, three complicated renal cysts, and seven simple renal cysts.

The mean enhancement of the renal cortex (or parenchyma) was 146, 150, and 88 HU during the cortical nephrographic, tubular, and pyelographic phases, respectively.

Of the solid-appearing lesions, the mean enhancement of RCC (n = 17) and other solid masses (n = 9) were 115 HU (95% confidence interval [CI]: 79–151 HU) and 51 HU (CI: −3–105), respectively. During the tubular nephrographic phase, the mean enhancements of solid-appearing RCC and other solid masses were 76 HU (CI: 57–96) and 54 HU (CI: 25–84), respectively. During the pyelographic phase, the mean enhancements were 49 HU and 35 HU. The difference in enhancement of RCC between the cortical nephrographic and tubular nephrographic phases was 39 HU, and the difference of mean enhancement of RCC between the cortical nephrographic and pyelographic phases was 66 HU, and 27 HU between the tubular nephrographic and pyelographic phases.

During the cortical nephrographic phase, the mean enhancement of the solid portion of the cystic RCC (n = 1) was 88 HU and 4 HU (CI: −2.6–11) for other cystic lesions (n = 10). During the tubular nephrographic phase, the mean enhancements were 44 HU and 7 HU (CI: 1.7–11.5), respectively. During the pyelographic phase, the mean enhancements were 29 HU and 7 HU, respectively. The difference of mean enhancement of the RCC was 44 HU between the cortical nephrographic and tubular nephrographic phases, 59 HU between the cortical nephrographic and pyelographic phases, and 15 HU between the tubular nephrographic and pyelographic phases. When all 18 RCC were considered, four (22%) demonstrated a maximum enhancement superior to that of the adjacent normal cortex during the cortical nephrographic phase (Fig. 1A–D), whereas seven (39%) were isodense to the renal cortex (±10 HU) (Fig. 2A–B). None of the other lesions (n = 19) was denser than renal cortex, and one oncocytoma was isodense to renal cortex. During the tubular nephrographic phase, one initially hyperdense RCC became

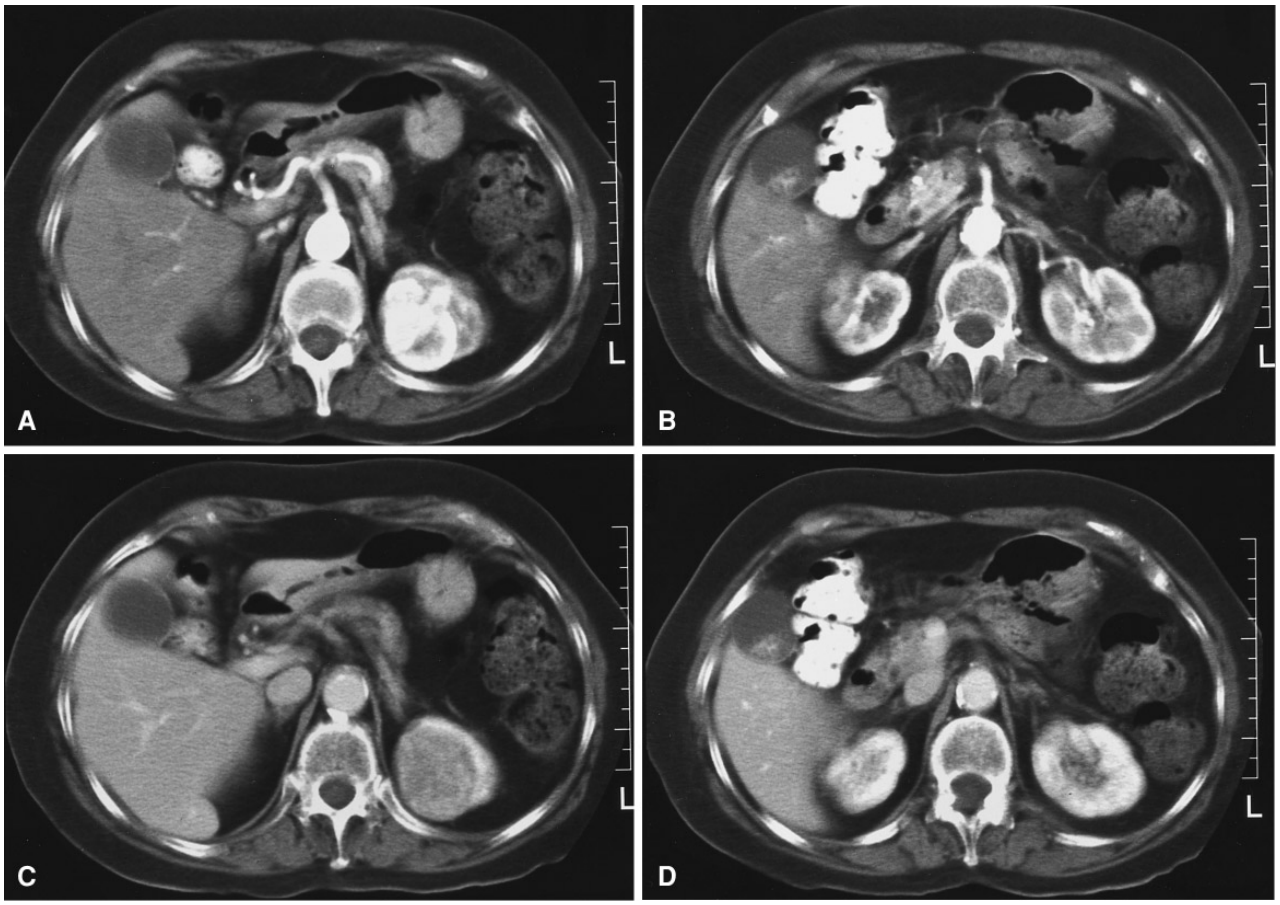

Fig. 1. Renal cell carcinoma. The mass is denser than normal cortex during the cortical nephrographic phase (**A, B**) and hypodense during the tubular nephrographic phase (**C, D**).

isodense to renal parenchyma, and the remaining three became hypodense. Six of the seven RCC that were isodense during the cortical nephrographic phase became hypodense to renal parenchyma, and one lesion remained isodense. The oncocytoma remained isodense to renal parenchyma during the tubular nephrographic phase (179 HU vs. 191 HU). Seven of 18 (39%) RCC were hypodense on both cortical nephrographic and tubular nephrographic phases. Hyperattenuation of a mass during the cortical nephrographic phase was 100% specific in diagnosing RCC but only 22% sensitive. Including both hyperattenuating and isoattenuating masses, the specificity was 92%, with a sensitivity of 61%. Comparing the maximal enhancement of renal masses during both cortical and tubular nephrographic phases, 12 of 18 (67%) RCC demonstrated a decrease in attenuation equal or superior to 10 HU, indicating wash-out of the intravenous contrast. Four lesions remained isodense (less than $\pm$10 HU variation), and two lesions had a higher attenuation value during the tubular nephrographic phase (Fig. 3A–B). On both cortical and tubular nephrographic phases, 16 of the 18 RCC (89%) were heterogeneous and two RCC (11%) were homogeneous. The presence of heterogeneous enhancement was therefore 89% sensitive in diagnosing RCC.

Combining the two previously described characteristics (hyper- or isoattenuation and heterogeneous enhancement) during the cortical nephrographic phase, 11 lesions were identified: 10 RCC and one oncocytoma, indicating a specificity of 91% and sensitivity of 56% of these combined findings in diagnosing RCC.

ROC curves (Fig. 4) demonstrated that the combination of the plain and cortical nephrographic phase acquisitions was similar or more accurate than the combination of the plain and tubular nephrographic phase acquisitions in diagnosing RCC. Combining all three acquisitions provided similar or more accurate results than any of the two other combinations individually and at all points (categories 1–5). This result explains the overlap of the curves as specificity decreases. Looking at a specific point of the ROC curves (category 4), a sensitivity of 85%, 90%, and 100% for the three combinations of phase acquisition, respectively, with a con-

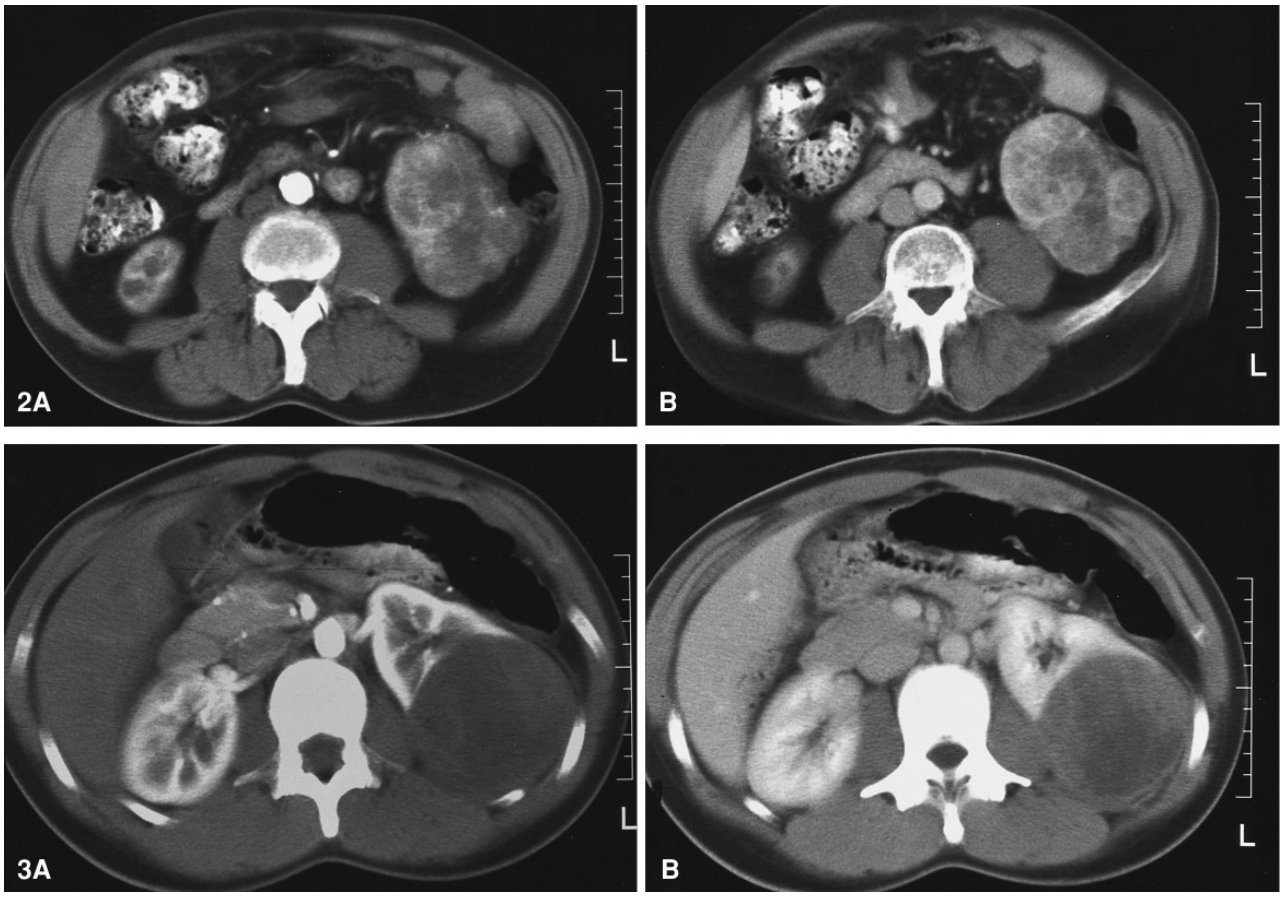

Fig. 2. Renal cell carcinoma. The mass is isodense to normal cortex during the cortical nephrographic phase (**A**) and hypodense during the tubular nephrographic phase (**B**).

Fig. 3. Renal cell carcinoma. The mass is hypodense to normal kidney during both cortical (**A**) and tubular (**B**) nephrographic phases. The mass is denser during the tubular nephrographic phase.

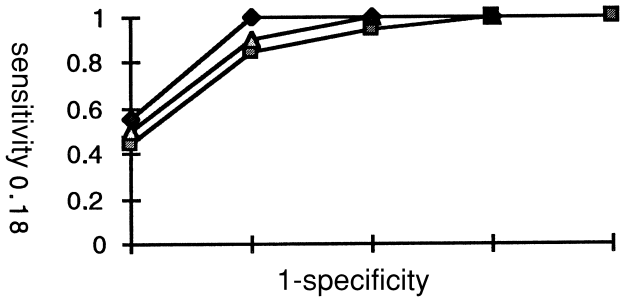

Fig. 4. ROC curves. (♦), PAV, three phases combined; (△), PA, plain and cortical nephrographic; (□), PV, plain and tubular nephrographic.

stant specificity of 88%, were obtained in the diagnosis of RCC.

Discussion

The expected pattern of enhancement of RCC during the cortical nephrographic phase, in keeping with the reported frequent hypervascularity of RCC, should be one of hyperattenuation [2, 4, 5, 11, 27]. This hypervascular appearance of RCC, mostly reported in the angiographic literature, is described in at least 80% of RCC. Studies of RCC with dynamic CT reported a 41–86% rate of hyperattenuating RCC during the cortical nephrographic phase of injection [28–30]. In two of these reports, the time delay after the initiation of intravenous contrast administration was less then 30 s, with a rate of infusion of 5 cc/s and 2 cc/s, respectively [28, 29]. In the third report, the time delay and rate of infusion were not specified [30]. Contrary to what was expected, hypervascularity, or hyperattenuation, to renal cortex during the cortical nephrographic phase acquisition was observed in only 22% of the 18 RCC included in our population, although all lesions but one were diffusely solid. RCC are also classically reported to demonstrate early wash-out of angiographic contrast material. In one series using dynamic CT, four of six hyperdense RCC became relatively hypodense (67%) and two became isodense (33%) during the tubular

nephrographic phase of CT scanning [28]. Even though no specific density measurements were provided, this suggests that six of six (100%) RCC included in that report demonstrated some degree of wash-out from the cortical nephrographic to the tubular nephrographic phase. With helical CT, this feature can only be demonstrated when a dual-phase acquisition (cortical and tubular nephrographic phases) is performed and is further amplified by the enhancement of the normal renal parenchyma [31]. Looking at the specific attenuation values of all RCC included in our population (n = 18), this wash-out phenomenon was present in only 12 (67%) lesions. Furthermore, two RCC had a higher attenuation value during the tubular nephrographic phase of excretion of intravenous contrast.

ROC curves were generated from data obtained from all 37 lesions (Fig. 4). Because most masses falling in category 4 (probably malignant) require an active management including at least clinical correlation (cases of abscesses) and possibly surgical exploration, analysis of the ROC curves was performed by using this category as the cutoff point. For these masses, the sensitivity and specificity for the plain and tubular nephrographic phases, plain and cortical nephrographic phases, and all phases combined to diagnose RCC were as follows: 85% and 88%, 90% and 88%, 100% and 88%, respectively. The addition of the cortical nephrographic phase increased the sensitivity to 100% when all phases were combined. The specificity remained at 88% for all three combinations. Even though the specificity of multiphasic helical CT appears unchanged when using category 4, the appearance of the ROC curves demonstrates that the combination of the plain and cortical nephrographic phase acquisitions was similar or more accurate than the combination of the plain and tubular nephrographic phase acquisitions in diagnosing RCC. Point-by-point analysis (categories 1–5) also revealed the superiority of the multiphase acquisition protocol over the two other combinations individually.

In our study, the optimal time interval between the administration of intravenous contrast and the first helical acquisition during the cortical nephrographic phase was not evaluated. Previous data obtained with dynamic CT showed that enhancement curves of normal cortex and medulla intersected at 47 s following initiation of contrast administration, when the rate of injection was 2.7 mL/s [31]. In one report on dynamic CT, where the rate of injection was 5 mL/s, the peak enhancement of normal renal cortex was reported to occur within 30 s [28]. In our protocol, high rate injection was favored because it was implicitly believed that it would reproduce an angiographiclike delivery of contrast to the kidney, therefore promoting the differential enhancement between RCC and normal cortex. This, however, remains a hypothetical advantage in favor of high rate injections in evaluating renal masses. Although the use of a multiphase helical acquisition increases the radiation dose delivered to the patient, we believe that the benefits in mass characterization outweigh the potential minimal increase in radiation-induced injury.

Conclusion

The cortical nephrographic phase provides unique and valuable information regarding the enhancement pattern of known renal masses, which is not available on a standard tubular nephrographic phase acquisition. Hyperattenuation of a renal mass during the cortical nephrographic phase was 100% specific for RCC in our population. Wash-out of intravenous contrast in a renal mass can only be appreciated with a dual-phase acquisition. The combination of the plain and cortical nephrographic phase acquisitions is more accurate than the combination of the plain and tubular nephrographic phase acquisitions in diagnosing RCC. Acquisition of images during the cortical nephrographic phase of intravenous contrast excretion improves the ability to accurately diagnose RCC when combined with the plain and tubular nephrographic phase acquisitions, with a sensitivity and specificity of 100% and 88%, respectively.

Therefore, the acquisition of a cortical nephrographic phase should be part of the routine helical CT protocol of renal masses.

References

1. McClennan BL. Computed tomography in the diagnosis and staging of renal cell carcinoma. *Semin Urol* 1985;3:111–131
2. Bosniak MA. Problems in the radiologic diagnosis of renal parenchymal tumors. *Urol Clin North Am* 1993;20:217–230
3. Wyatt SH, Urban BA, Fishman EK. Spiral CT evaluation of the kidney. In: Fishman EK, Jeffrey RB (eds). *Spiral CT: principles, techniques and clinical applications.* New York: Raven Press, 1995:87–107
4. Curry NS. Small renal masses (lesions smaller than 3 cm): imaging evaluation and management. *AJR* 1995;164:355–362
5. Newhouse JH. The radiologic evaluation of the patient with renal cancer. *Urol Clin North Am* 1993;20:231–246
6. Malkowicz SB. Clinical aspects of renal tumors. *Semin Roentgenol* 1995;30:102–115
7. Bosniak MA, Rofsky NM. Problems in the detection and characterization of small renal masses. *Radiology* 1996;198:638–641
8. Lange S (ed). Diseases. In: *Teaching atlas of urologic radiology.* New York: Thieme Medical Publishers, 1995:49–177
9. Davidson AJ, Hartman DS (eds). Diagnostic set: Large, unifocal, unilateral. In: *Radiology of the kidney and urinary tract,* 2nd ed. Philadelphia: WB Saunders, 1994:327–403
10. Bosniak MA. The small (≤3.0 cm) renal parenchymal tumor: detection, diagnosis, and controversies. *Radiology* 1991;179:307–317
11. Bosniak MA. The current radiological approach to renal cysts. *Radiology* 1986;158:1–10

12. Birnbaum BA, Bosniak MA, Krinsky GA, et al. Renal cell carcinoma: correlation of CT findings with nuclear morphologic grading in 100 tumors. *Abdom Imaging* 1994;19:262–266
13. Hartman DS, Weatherby E III, Laskin WB, et al. Cystic renal cell carcinoma: CT findings simulating a benign hyperdense cyst. *AJR* 1992;159:1235–1237
14. Levine E. Renal cell carcinoma: clinical aspects, imaging diagnosis, and staging. *Semin Roentgenol* 1995;30:128–148
15. Herts BR, Einstein DM, Paushter DM. Spiral CT of the abdomen: artifacts and potential pitfalls. *AJR* 1993;161:1185–1190
16. Zeman RK, Fox SH, Silverman PM, et al. Helical (spiral) CT of the abdomen. *AJR* 1993;160:719–725
17. Chernoff DM, Silverman SG, Kikinis R, et al. Three-dimensional imaging and display of renal tumors using spiral CT: a potential aid to partial nephrectomy. *Urology* 1994;43:125–129
18. Birnbaum BA, Jacobs JE. Multiphasic renal CT: comparison of renal mass enhancement during the corticomedullary and nephrographic phases. *Radiology* 1995;197(P):147
19. Merran S (ed). Technique. In: *Rein et Tomodensitométrie*. Paris: MEDSI, 1986:22–23
20. Sherman LS, Cohan RH, Korobkin MT, et al. Spiral CT of renal masses: assessment of corticomedullary and nephrographic phase images [abstract]. *Radiology* 1994;193(P):135
21. Silverman PM, Cooper CJ, Weltman DI, et al. Helical CT: practical considerations and potential pitfalls. *RadioGraphics* 1995;15:25–36
22. Kopka L, Zoeller G, Schmidt C, et al. Helical CT of the kidneys in the corticomedullary and nephrographic contrast phases: detection of renal masses and staging of renal cell carcinoma. *Radiology* 1995;197(P):147
23. Kauczor HU, Schwickert HC, Schweden F, et al. Bolus-enhanced renal spiral CT: technique, diagnostic value and drawbacks. *Eur J Radiol* 1994;18:153–157
24. Davidson AJ, Davis CJ Jr. Fat in renal adenocarcinoma: never say never. *Radiology* 1993;188:316
25. Strotzer M, Lehner KB, Becker K. Detection of fat in a renal cell carcinoma mimicking angiomyolipoma. *Radiology* 1993;188:427–428
26. Hélénon O, Chrétien Y, Paraf F, et al. Renal cell carcinoma containing fat: demonstration with CT. *Radiology* 1993;188:429–430
27. Foster WL Jr, Roberts L Jr, Halvorsen RA Jr, et al. Sonography of small renal masses with indeterminant density characteristics on computed tomography. *Urol Radiol* 1988;10:59–67
28. Tada S, Fukada K, Aoyagi Y, et al. CT of abdominal malignancies: dynamic approach. *AJR* 1980;135:455–461
29. Zeman RK, Cronan JJ, Rosenfield AT, et al. Renal cell carcinoma: dynamic thin-section CT assessment of vascular invasion and tumor vascularity. *Radiology* 1988;167:393–396
30. Zagoria RJ, Wolfman NT, Karstaedt N, et al. CT features of renal cell carcinoma with emphasis on relation to tumor size. *Invest Radiol* 1990;25:261–266
31. Ishikawa I, Onouchi Z, Saito Y, et al. Renal cortex visualization and analysis of dynamic CT curves of the kidney. *J Comput Assist Tomogr* 1981;5:695–701